IEEE Robotics and Automation Letters (RAL) paper presented at the
2020 IEEE/RSJ International Conference on Intelligent Robots and Systems (IROS)
October 25-29, 2020, Las Vegas, NV, USA (Virtual)

Retraction Mechanism of Soft Torus Robot with a Hydrostatic Skeleton

Tomoya Takahashi, Masahiro Watanabe, Kenjiro Tadakuma*, Masashi Konyo and Satoshi Tadokoro,
Tohoku University

***Abstract*—Soft robots have attracted much attention in recent years owing to their high adaptability. Long articulated soft robots enable diverse operations, and tip-extending robots that navigate their environment through growth are highly effective in robotic search applications. Robots that extend from the tip can lengthen their body without friction from the environment. However, the flexibility of the thin membrane inhibits the retraction motion of the tip due to buckling. Two methods have been proposed to resolve this issue; increasing the pressure of the internal fluid to reinforce rigidity, and mounting an actuator at the tip. The disadvantage of the former is that the increase is limited by the membrane pressure resistance, while the second method leads to robot complexity. In this paper, we present a tip-retraction mechanism with a hydrostatic skeleton that can prevent buckling and takes advantage of the friction from the external environment. water is used as the internal fluid to increase ground pressure with the environment, which is different from the conventional methods that use pneumatic. We explore the failure pattern of the retraction motion and propose solutions by using a hydrostatic skeleton robot. Additionally, we develop a prototype robot that successfully retracts by using the proposed methodology. Our solution can contribute to the advancement of mechanical design in the soft robotics field with applications to soft snakes and manipulators.**

***Keywords*—Soft Robot Materials and Design, Mechanism Design**

I. Introduction

In recent years, soft robots have received increasing attention. Particularly, long multi-segmented robots are highly articulated to enable diverse operations (e.g., varied tasks, wide-range movement) [1] and applications (e.g., robot arms and snake-type robots) [2]–[4]. Additionally, articulated robots can deform the robot to a smaller radius of curvature by increasing the number of joints, shortening the length of each joint, and increasing the overall length. For example, in a search robot navigating in a narrow area, the higher the curvature is, the more the movement range increases. If a long segmented robot is composed of a soft body, it can be regarded as a highly articulated and extremely small link and can be deformed with a higher curvature [5][6][7].

Among long soft robots, tip-extending robot have been proposed [8]–[11] and have shown high effectiveness, especially in the field of search robotics. Tip-extending robots carry a mechanism that allows the membrane to grow from the endpoint. The advantage of this mechanism is that the tip can extend without friction from sliding against the environment.

Tomoya Takahashi, Masahiro Watanabe, Kenjiro Tadakuma, Masashi Konyo, and Satoshi Tadokoro are with the Graduate school of Information Sciences, Tohoku University, Japan (*Corresponding author: Kenjiro Tadakuma (email: tadakuma@rm.is.tohoku.ac.jp).).

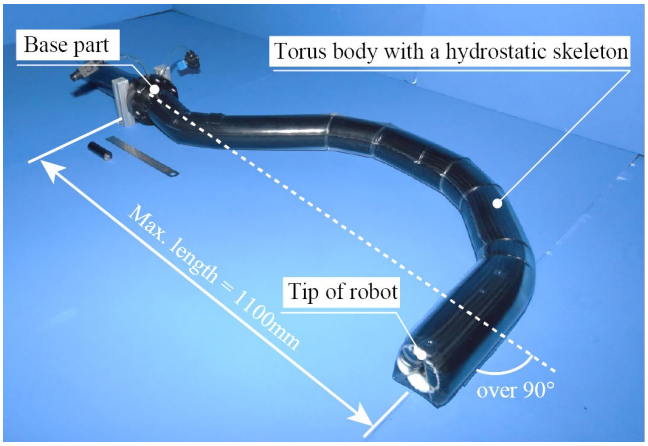

Fig. 1 The torus-type robot we proposed can retract its body from the tip even if it curves over 90°.

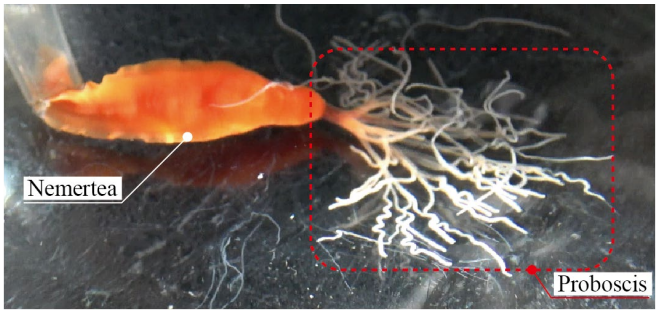

Fig.2 Nemertea has a tip-extending mechanism in their proboscis that can branch, extend, and bend. They can also retract their proboscis by pulling it from the tip. (This picture was taken by Kajihara lab in Hokkaido University)

However, these robots have a problem that it is difficult to retract from the tip because the membrane of the robot consists of a soft sheet, which is strong in the tensile but extremely weak in the compressive. Thus, buckling occurs when wire tension is applied from the root to the tip. Since these robots can not retract, it is impossible to go backward and re-select the path. In addition, it may disrupt the environment when simply pulling out the robot from a fragile and narrow area. In our laboratory, we also focus on the realization of branched growing structures [12] for safe and efficient searching. Although several branching structures have been proposed [13][14], these structures are more difficult to retract because of their intricate shapes.

On the other hand, Creatures, such as some type of Nemertea, have been reported to carry a tip-extending

mechanism in their proboscis that can branch, extend, bend, and retract (Fig.2) [15]–[18]. They use this structure not only for predation, but also for locomotion. The proboscis with a complex shape and multiple extending tips are considered to provide a simple structure for the retraction without the complicated control. If we could reproduce the Nemertea proboscis as a soft robotic mechanism, it would be possible to realize a simpler retraction structure than the conventional one. In this paper, we focused on the fact that a Nemertea lives underwater and operates its proboscis by liquid instead of air, which is widely used in previous tip-extending robots. Further, we analyze the deformation modes when retracting the tip of a simple straight tip-extending robot.

The main contributions of this study are the exploration of the retraction fails modes of a torus-type tip-extending robot and the conditions for its occurrence and the development of a method that prevents buckling even when the robot body is composed of a soft membrane. This paper is structured as follows. In Section II, we discuss the factors that cause buckling and study the mechanical conditions of the retraction. Section III presents the development of a prototype design. In Section IV, we perform experiments to validate the effectiveness of the proposed mechanism. In Section V we discuss the result of the experiment and the problem of the proposed method. In Section VI, includes our conclusions and scope of future work.

II. Basic Principle

The several methods to retract of torus mechanism and analysis of failure condition of retraction have been proposed. Coad et al[19]. measured the force required to pull the inner membrane for the retraction and analyzed the failure pattern to retract the curved torus body. This analysis shows that the growing robot tends to buckle even when the robot is slightly bent, and the length of possible retraction by pulling the inner membrane decreases as the curvature increases. Coad et al. [19] and Jeong et al. [20] have solved this problem by installing an actuator at the tip. These failures are due to the very low stiffness of the inflatable beam made of thin membrane and it shows there is a limit to the increase in stiffness by pressurization. Even if it is possible to increase the rigidity by applying pressure, the body also returns to a straight shape and can not retract with keeping a smoothly curved shape.

Another method found in common among conventional robots is that they use air as the internal fluid. On the other hand, a method found in nature, such as Nemertea, which has succeeded in reverting to a complex branched torus structure, forms a hydrostatic skeleton by filling the soft membrane of proboscis with water. We consider there are some advantages to a successful retraction for the tip extending mechanism. Loung et al. proposed a water filled growing robot[21], but they limited it to use in water where neutral buoyancy can be achieved, and did not focus on the fact water has higher specific gravity than air and it can fill the interior at low pressure due to its incompressibility.

In this study, we propose a new method to retract by using a hydrostatic skeleton successfully according to the increase of the maximum frictional force by changing the internal fluid to water with high specific gravity and increasing the contact

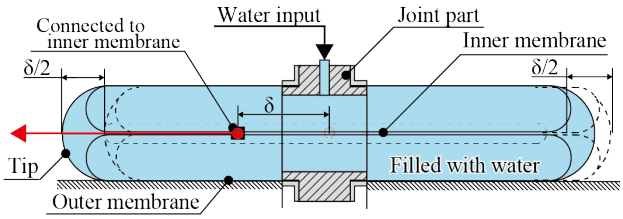

Fig.3 Schematic of a torus tip-extending robot

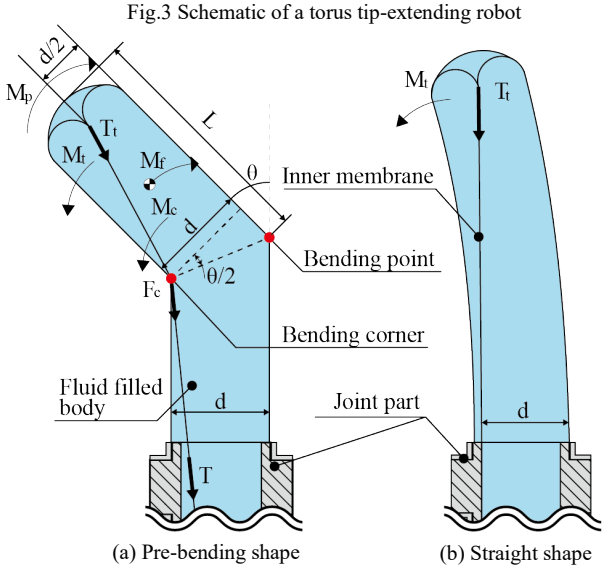

Fig.4 Free body diagram with the forces acting on the torus body

force with the ground to maintain the posture. By using water as the internal fluid, the force of contact with the ground increases, and the posture can be kept by friction with the ground surface while retracting the robot's body. In this paper, we assumed operation in a 2D plane where the underside of the membrane is always in contact with the ground and found deformation modes and the conditions of failure retraction under which they occur when a linear torus robot is bent on the ground. This method has two advantages: The path of the robot is not straight but has a smooth curve because the interior can be filled with low-pressure water. Additionally, this solution simplified the structure of the robot, especially if it is branched.

A. Prototype and model

Fig. 3 shows the structure of a torus-type tip-extending robot. Both ends of the robot are folded back from the outer to the inner membrane. The inner membrane is connected on the inside, while both ends of the outer membrane are fixed to the center joint. When the inner membrane is pulled by a factor δ to the left, the length of the right side contracts by $\delta /2$, and the left side extends by $\delta /2$, as illustrated in Fig. 3. Then, a joint is provided in the middle to connect with the outer membrane, and the inside is filled with fluid injected from the joint. The torus-robot used in this paper has a wire welded to the inner membrane, which can be contracted and extended only in one direction by applying tension by wire as shown in Fig. 3 (details are described in Sections III-A and IV-A). Although this robot is limited to unidirectional movement to perform experiments on retraction, it is possible to drive in both directions by methods such as attaching a rod to the inner membrane as proposed by Haili et al [22]. Future methods of actuating are described in the discussion.

By symmetrically connecting the two tip-extending structures, we achieve certain advantages compared to the single mounting structure. First, since there is no volume change while the robot moves, there is no pressure change when retracting. Second, the force required for contraction is small and constant because tension is applied to both ends of the inner membrane and is thus balanced.

Conventionally, robots are pneumatically driven, but in this paper, we use water as the internal fluid. Therefore, the lower side of the outer membrane is always in contact with the ground surface owing to the added weight. This is discussed in detail in Section II-C (iii).

B. Moments acting on the torus body

The straight torus-type robot presented in the previous section can be bent in the middle while keeping its shape owing to friction from the ground because the pressure of the working fluid is low and ground pressure is large. Fig. 4 shows the free body diagram when the elbow of the robot is retracted from the tip. The moments generated in the body are discussed as follows.

Note that the model assumes a circular cross section, and the inner membrane can be regarded as a wire without volume. It is also assumed that the membrane does not expand or contract owing to the generated force.

(i.) M_t *: Bending moment owing to tip tension T*

When tension T_t is generated at the tip as shown in Fig. 4 and Fig.6 (a), the moment M_t occurs around point O is described as

$$M_t = r_t \cdot T_t = \frac{dLT_t}{\sqrt{(d/2)^2 + L^2}}, \quad (1)$$

where d is the diameter of the body, L is the length between O to the tip of the body. Then, T_t is the pressure multiplied by the cross-sectional area

$$T_t = \frac{\pi p d^2}{4}. \quad (2)$$

M_t can be expressed as

$$M_t = \frac{\pi p L d^3}{4\sqrt{(d/2)^2 + L^2}}. \quad (3)$$

(ii.) M_c*: Bending moment owing to friction generated at the bending corner*

When the inner membrane is bent along the bending corner, the bending moment is generated by the capstan friction. According to Euler's belt theory, when the inner membrane bent at a pre-bending angle θ starts to slip, the tension T_b at the base is

$$T_b = T_t e^{\mu_b \theta}, \quad (4)$$

Where μ_b is the coefficient of friction between membranes. The force F_c applied from the inner to the outer membrane can be expressed as follows

$$F_c = T_b - T_t = T_t\left(e^{\mu_b \theta} - 1\right). \quad (5)$$

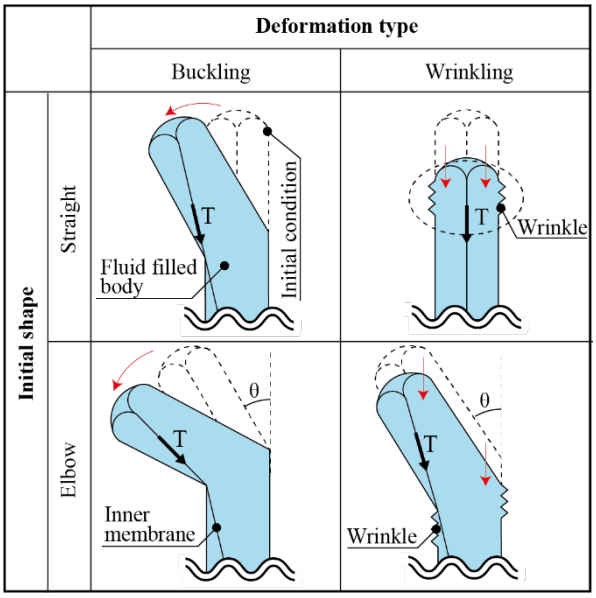

Fig.5 Modes of torus robot deformation

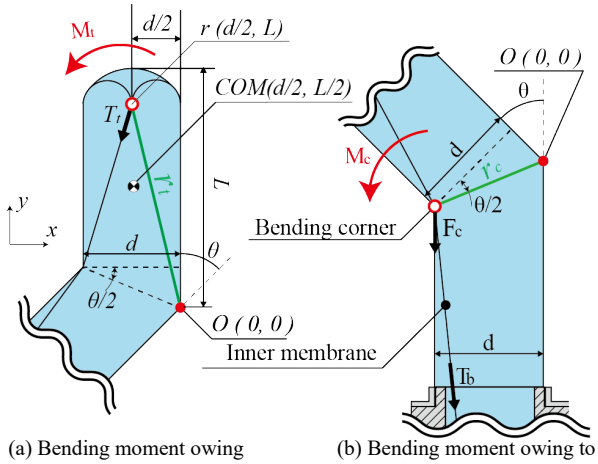

(a) Bending moment owing to tip tension

(b) Bending moment owing to corner friction

Fig.6 Schematic of bending moment

If the base side of the robot is sufficiently long, F_c can be working in parallel with the outer membrane at the root, so the bending moment M_c owing to friction is given as follows

$$M_c = F_c \frac{r_c}{cos(\theta/2)} = F_c d = \frac{\pi p d^3}{4}\left(e^{\mu_b \theta} - 1\right), \quad (6)$$

where Rc is the moment arm of Mc as shown in Fig.6.

(iii.) M_f*: Moment of resistance generated by friction with the ground*

The maximum value of the bending moment owing to friction is expressed by the following equation.

$$M_{fmax} = \frac{\rho \mu g L^2}{2}, \quad (7)$$

Where ρ, μ, g are the mass of the body per unit length, the coefficient of friction between the body and the ground, and the gravitational acceleration, respectively.

(iv.) M_p: *Moment to return to a straight line by pressure*

When the inner of an elbow-shaped torus body is filled with water, the hydraulic pressure effects the body to return to a straight shape. In this case, the following moment occurs [23][24]

$$M_p = T_t \frac{d}{2} = \frac{\pi p d^3}{8}. \tag{8}$$

C. Modes of deformation

It was found that the mode of retraction failure was not uniform but changed to various shapes just by pulling the inner membrane when the torus-type tip-extending robot was operated with water. Through experiments, we found that the deformation pattern of the robot was determined by its initial shape. The classification of this deformation pattern and its cause are summarized below.

(i.) Straight-buckling

In this phenomenon, The force F_{cr} applied to the tip at the onset of buckling is expressed as[25][26]

$$F_{cr} = \frac{EI\frac{\pi^2}{L^2}(p\pi r^2 + G\pi rt)}{EI\frac{\pi^2}{L^2} + p\pi r^2 + G\pi rt}, \tag{9}$$

where *E, I, G* are Young's module, second moment of area of the body, and the shear module, respectively.

However, when the body is curved at a constant curvature, as shown in Fig. 4(b), the moment is generated in the direction in which the body is curved and bent. The moment T_t from the tension applied to the tip of the robot generated at this time is expressed as

$$M_t = T_t d. \tag{10}$$

Moreover, if the distance from the bending corner to the tip is L, buckling occurs at the base when $M_t > M_f$, so the equation of T_t at which bend occurs is expressed as

$$T_t > \frac{\rho\mu g L^2}{2d}. \tag{11}$$

This mode was not confirmed when using water as the internal fluid and operating at low internal pressure and high ground pressure, but it was observed when the air was injected at high pressure.

(ii.) Straight-wrinkling

When tension is applied to the inner membrane, bellow-like deformation occurs before the tip folds back. This phenomenon occurs at low pressure, contrary to (i). when the force F_w applied to the robot tip, the pressure needs to satisfy the below equation to prevent wrinkling[27]

$$p \geq \frac{2F_w L}{\pi r^3}. \tag{12}$$

(iii.) Elbow-buckling

This is a phenomenon in which θ becomes larger when a force is applied to the inner membrane of the body that is originally bent at an angle θ. Once bend occurs, θ increases and the retraction fails. The condition under which buckling occurs at a pre-bending angle θ is determined by the distance L from the bending point. The derivation of this condition is as follows. First, when the body is buckled, the forces applied to it are as shown in Fig. 3. At this time, the condition that the tip of the body slips can be expressed by the balance of the moments around bending point O in Fig. 6

$$M_t + M_c > M_{fmax} + M_p. \tag{13}$$

To prevent elbow-buckling, it is conceivable to increase M_f or decrease M_t,M_c. In this study, this was done by using water as the internal fluid because the density ρ is increased when using water compared to using air. Additionally, the incompressible nature of water, enables filling the interior with liquid at low pressure, so that the tensions T_t reduced and M_t becomes smaller than M_f.

(iv.) Elbow-wrinkling

When the body bends at large angles, the force applied to the bending corner and base increases, and the body is wrinkled at the base before buckling or retracting. Simultaneously, the tip of the body rotates in the direction in which θ decreases. When the force F_c generated at the bending corner is applied and the tip of the body of length L slips. the following relationship is established as the balance of the moment around tip:

$$F_c L cos\theta > M_{fmax} = \frac{\rho\mu g L^2}{2}, \tag{14}$$

$$F_c > \frac{\rho\mu g L}{2cos\theta}. \tag{15}$$

The condition for generating elbow-wrinkling is expressed by the following equation:

$$F_c > \frac{\rho\mu g L}{2cos\theta} + F_w. \tag{16}$$

Therefore, for elbow-buckling to occur, the bending angle θ and the bending tip length L must satisfy the following formula:

$$F_c = T_t\left(e^{\mu_b\theta} - 1\right) > \frac{\rho\mu g L}{2cos\theta} + F_w. \tag{17}$$

D. Retract through the bending point

So far, we have described the retraction method from the tip to the bending point. In this section, we focus on the method of retraction through the bending point. The elbow-buckling discussed in the previous section can be avoided by reducing the pre-bending angle. However, the condition we calculated indicates that the elbow-bend always occurs during the retraction process. The reason is that independent of whether the pre-bending angle diminishes or whether the retraction is successful, L approaches 0. Consequently, M_f becomes smaller than the bending moment. To avoid this phenomenon, it is necessary to increase the pressure and corresponding moment M_p. However, there is a limit to the increase in pressure as explained in section I. Therefore, in this study, the strength when L is small was reinforced by a mesh tube to successfully retract the tip through the bending part. The

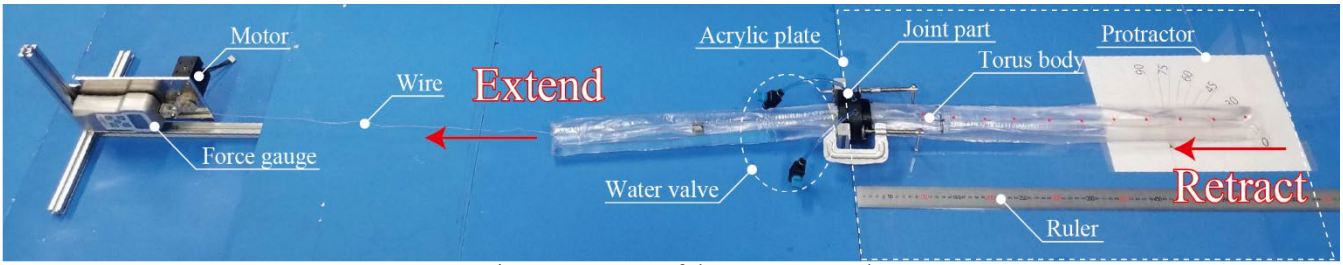

Fig. 7 Prototype of the torus-type robot

method is also explained in detail in section III-B. When the mesh tube was inserted into the torus robot, the condition that elbow buckling starts is described as below

$$M_t + M_c > M_{fmax} + M_p + M_{tube}.$$

Where M_{tube} is the restoring moment of mesh tube and monotonically increases to the bending angle theta.

E. Extending theory for the multi-bending structure

The conditions for the deformation described in Section II can also apply to the torus body that has multiple bends. In this case, buckling likely occurs at the bending point. Therefore, the multi-bending torus structure can be considered as multiple rigid links, as shown in Fig. 8. In this case, the condition for the n_{th} link to rotate is

$$M_n > M_{n-1} + \mathrm{M_{n+1}}, \tag{18}$$

where M_{n-1} and M_{n+1} are moments of $(n-1)_{\text{th}}$ and $(n+1)_{\text{th}}$ links to the n_{th} link, respectively. Then, M_n is calculated from the Eq. (11)

$$M_n = M_{fmax} + M_p + M_{tube} - M_{cn}, \tag{19}$$

where M_{cn} is the moment around O due to the corner Force F_{cn} and F_{cn+1}. By using Eqs. (10) and (18), M_{cn} and F_{cn}can describe as follows.

$$M_{cn} = (F_{cn} + F_{cn+1})d, \tag{20}$$

$$F_{cn} = F_{cn+1}\left(e^{\mu_b \theta n} - 1\right). \tag{21}$$

By (21) and (22), It is clear that M_{cn} can be reduced by reducing the bending angle θ_n at each bend. Therefore, if the number of bends increase and the curvature is sufficiently small in the multi-bend structure, as shown in Fig. 1, it is possible to retract from a bend of 45 degrees or more, which was not possible with a single bend.

III. Mechanical Design

A. Torus-type robot with hydrostatic skeleton

The first prototype of the proposed torus-type robot shown in Fig. 7 was made for performing our experiments. A 0.1 mm polyurethane sheet was used as a flexible material, and two sheets were welded and formed into a tube. This polyurethane tube was folded back to form a torus structure. The ends of the outer membrane were connected with a joint made by a 3D printer. Then, water was injected into the tube from the joint. The dimensions of the body of the robot are shown in Table I.

B. Torus-type robot with reinforced hydrostatic skeleton

To make the torus-type robot less likely to buckle, we designed a growing robot inserted a guide tube with a low coefficient of friction as shown in Fig.9. This robot is composed of the torus robot with hydrostatic skeleton and

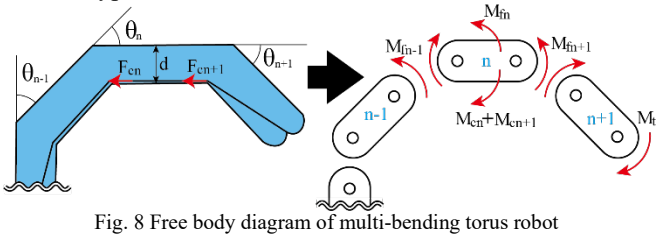

Fig. 8 Free body diagram of multi-bending torus robot

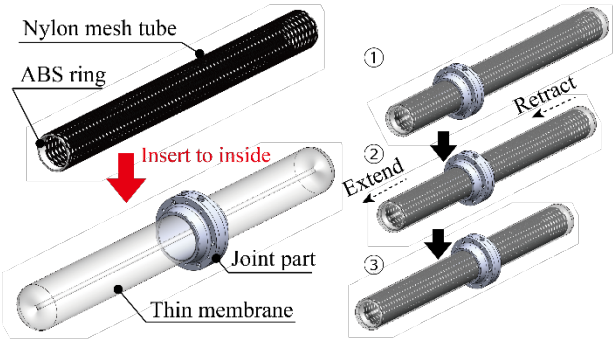

(a) Structure of torus robot (b)Extend and retract movement

Fig.9 Torus-type robot with reinforced hydrostatic skeleton

TABLE I. Dimensions of the Body of the Torus Type Robot

Length	Diameter	Weight	Wire diameter
1100 mm	50 mm	2318 g (at 100%)	0.6 mm

cylindrical mesh tube inserted inside of the robot covering the inner membrane. This tube is not folded in a torus shape like the membrane but moves inside the robot while sliding with the inner membrane according to the robot's movement.

This structure has two advantages compared to the prototype. First, a reduction in friction between the membranes is achieved. As described in Section II-A, it is important to reduce the friction at the bending part for reducing the bending moment. Second, the stiffness of the robot is increased by adding the tube. The guide tube is made out of a high stiffness material, stiffer than that of the membrane, because it does not need to be folded back and must keep its shape while the robot moving. Additionally, to reinforce the body to prevent deformation, we added a nylon mesh tube. It was used to reduce the friction surface of the robot because of its low friction and flexibility[28]. Nylon was selected as the material because it is slippery and can bend greatly while maintaining radial strength. The mesh tube was inserted while compressing it in the longitudinal direction by half the length. It can be extended to the length of the mesh tube to be the same as the robot owing to its high elasticity. Furthermore, an ABS ring made by a 3D printer was fixed to both ends of the mesh tube to prevent it from being folded.

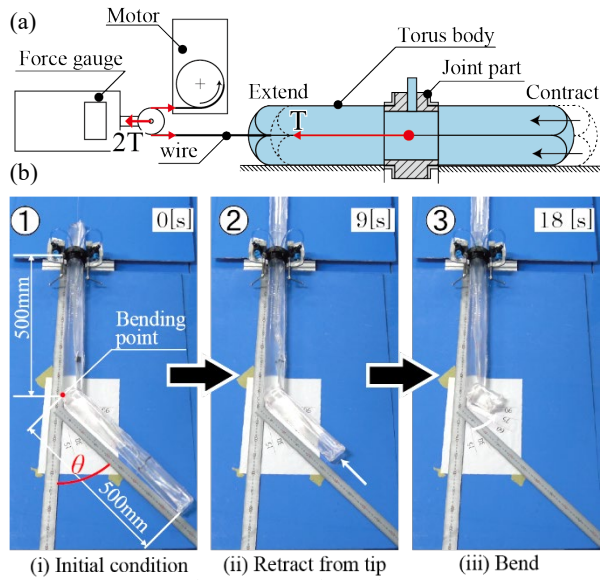

Fig.10(a) Experimental set up;
(b) Measurement of tension at elbow shape

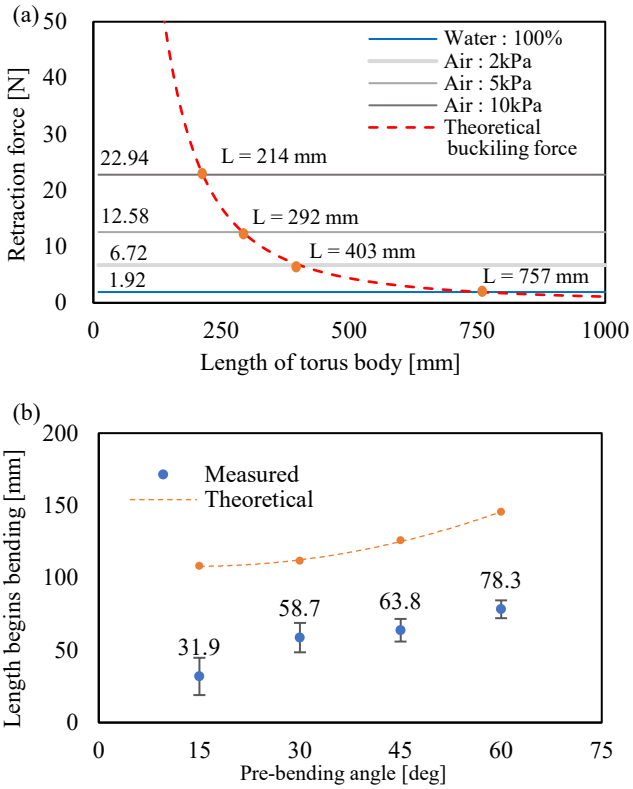

Fig. 11 (a) Comparison between the retraction force and buckling force;
(b) Buckling start length.

IV. Experiment with Prototype Model

A. Experimental setup

The experimental setup is illustrated in Fig. 10(a). A wire is welded to the center of the inner membrane of the torus-type robot and is connected to the motor (Dynamixel XH540-V150-R, South Korea) via a pulley attached to the force gauge (FGP-5, Nidec-Shimpo Corp., Japan). When the motor was rotated and the wire was wound twice, wire tension was applied to the force gauge. We logged this tension until the motor stopped.

In this experiment, we used the volume filling rate to measure the filling amount of water inside the robot. The volume filling rate is defined as the ratio of the water volume to the maximum volume, which is estimated from the model described in III-A as 100%. This volume is measured by the mass of the water inside the robot. Note that the volume filling rate can be more than 100% because the film can stretch. In this paper, we experimentally verify the conditions for the generation of straight-buckling and elbow-buckling. Because wrinkling is easy to prevent by applying high pressure.

B. Results

(i.) Retraction force measurement at straight-buckling

To verify the straight-wrinkling conditions explained in II-C, we measured tension needs to retract the torus body caused by the difference in the water filling rate. We set up the torus-type robot as shown in Fig. 10 (a) and (b) to measure the tension. Then, we fixed the joint to the ground and let one side of the body rest on the acrylic plate. The body can keep its elbow shape owing to the friction from the acrylic plate. In this experiment, the initial shape was such that the body was bent at 500 mm from the joint and the length from the bending point to the tip was 500 mm. When the motor rotated at a constant speed (approx. 44 mm/s), the wire connected to the robot, and the motor pulled the inner membrane to folded back the tip. When measuring the air-injected types, square pipes were placed as guides on both sides to prevent buckling.The tension was measured with a force gauge, and the average value of the tension for 10 seconds after applying the tension was defined as the tension T_m applied to the inner membrane. We measured the tension at a pre-bending angle of 0 deg. In this robot configuration, the tension applied to the inner membrane by the pressure balances at both ends. Therefore, no force should be required for the robot to deform, but the tension T_m, which is required to move the robot, is measured. This is the force required for the transition from the outer membrane to the inner at the edge of the torus structure while creating wrinkles. The tip tension T_t is expressed in the following equation

$$T_t = \frac{\pi p d^2}{4} + T_0, \tag{22}$$

where T_0 is the measured retraction force when the pre-bending angle is 0 deg.

Fig. 11 (a) shows the retraction force measured in the experiment when the air pressure is 2 kPa, 5 kPa, and 10 kPa and 100% volume filling of water. The theoretical buckling force is calculated by Eq. (9). In this equation, the value of Young's modulus and shear modulus of polyurethane were 23 MPa and 30 MPa, respectively. This theoretical value does not change significantly with pressure. For example, the difference between the model of 244 Pa of water calculated by Eq.(8) and 10 kPa of air is only 0.01%. Therefore, we can compare the water-filled model and air-filled model in the same graph shown in Fig. 11 (a). This figure shows the lengths of buckling may occur without ground friction at 2 kPa, 5 kPa, 10 kPa, and 100% water were L = 403 mm, 292 mm, and 214 mm, 757 mm respectively. Actually, the water-filled version can retract without buckling when L = 1000 mm.

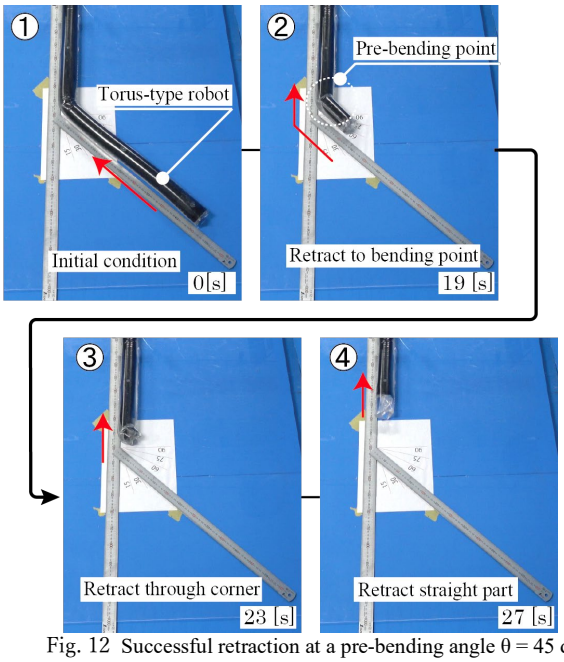

Fig. 12 Successful retraction at a pre-bending angle θ = 45 deg

TABLE II. SUCCESS RATE OF RETRACTION THROUGH THE BENDING POINT

Only water		15deg	30deg	45deg	60deg
	100%	0	0	0	0
	110%	100	0	0	0
	115%	100	0	0	0
	120%	100	0	0	0
With guide tube		100	100	30	0

(ii.) Bend start length measurement at elbow-buckling

The elbow-buckling condition explained in II-C was experimentally verified. In this experiment, we measured retracting force and buckling length L in the same experiments in (i). Retraction stopped when the body bends. In this case, the length L was measured by measuring the length between the point O and the tip when the retraction was stopped after confirming the robot buckled. Since L does not change after buckling occurs, the length at this time considered to be L. It was determined the average of 10 measurements.

Fig. 11 (b) shows a comparison between the measured and theoretical value of the bending start length obtained from Eq. (13). The coefficient of friction between the acrylic plate and the polyurethane was 0.81, which was experimentally measured using a pouch made of the same material as the robot and filled with a constant mass of water. This pouch was attached to the experimental installation shown in Fig. 10(a), and the coefficient of friction was calculated by measuring the maximum force required to start sliding when pulled by wire using a force gauge. And M_c is calculated as shown below

$$M_c = F_c d = (T_m - T_t)d. \tag{23}$$

(iii.) Success rate of retraction through the bending point

To verify the effectiveness of the guide tube for retraction through the bending point described in II-D, we compare the success rate for retracting (Table II). It was calculated as the number of successful retractions through the bending point among 10 trials, as described in (i). Fig. 12 shows the retract operation (also show in the supplementary video).

V. DISCUSSION

A. Analysis of experimental results

Through this study, we present practical findings regarding the retraction failure modes and a design method that aims to improve the success rate of retraction in a tip-extending robot. Fig 11(a) shows the comparison of buckling conditions between air and water. In general, if the robot is more extended, it must buckle. However, we found that in the case of water, the buckling is not likely to occur owing to the low retraction force and the large ground friction. For that reason, the buckling of a long state can be prevented. Also, shown in Fig.11 (b), we found that the length at which the buckling started was shorter than the theoretical value. In this model, we assume that there is no membrane elongation while buckling. However, the membrane needs to stretch at the bending point during buckling. Therefore, the moment necessary to deform and buckle the membrane is needed on the right side of Eq (13). The model can be more accurate by including all these considerations.

As can be seen from Table II, the robot with a guide tube could be retracted to 45 deg without buckling 30% of trails. It is thought that the moment is balanced, as shown in Eq. (20), and that the wrinkles cause the variation in the corners. On the other hand, the success rate of the retraction did not change even inner pressure was increased. This is because the pressurizing occurs not only increases M_p in equation (13), but the increase M_t and M_c by increasing retraction force T_t. But by using a guide tube, it can reinforce the robot and reduces M_c by decreasing friction between membranes at the bending corner without affecting the retraction force. Though the robot can retract only when its bending angle is smaller than 45 deg, the multi-bend structure enables the robot to retract from a larger angle as shown in II-E. However, since this method cannot change the direction of the robot with a large curvature, it is necessary to improve to retract from a larger bending angle, as explained in the following section.

B. Improvement approach and limitation of proposed method

We suggest the following three methods for improving the success rate for tip retraction. (i) Reduce the friction at the bending point to limit buckling and wrinkling by changing to a more stretchable membrane material or a guide tube material with a low coefficient of friction. (ii) Increase the density of the inner fluid to increase the ground pressure between the robot and the ground to prevent slippage. (iii) Reinforce the guide tube to support body stiffness by choosing a stiff and slippery material and further compressing the guide mesh tube.

However, this method has the following problems. First, once buckling has occurred, there is no way to make it straight again. Once the robot buckles, a stronger force requires because of friction moment. Secondly, in the case of hydraulic systems, there is a problem that the fluid cannot be compressed and stored in a small container in comparison with pneumatic systems. Lastly, there is a restriction to 3D space. Due to the increased specific gravity of the internal fluid, only the stiffness of the membrane cannot hold the weight of the robot body. Also, since this method retains its shape by friction with the ground, it is considered to be challenging to perform the same movement in air or water where it does not make contact

with the ground. However, it may be possible to operate on a slope by applying high pressure.

VI. Conclusion

Summing up, in this study, we investigated the retraction failure through theoretical calculations and experimental procedures based on torus body tip-extending robot design. Additionally, we derived the conditions for the occurrence of buckling and bending. It was found that the retraction failed when the bending moment from internal tension exceeded the maximum resistance moment from the friction between the membrane and the environment.

Further, we proposed three methods for successful retraction: (1) Increase the resistance moment from friction with the external environment, (2) Minimize the internal frictional resistance as much as possible, and (3) Reinforce the robot body by inserting a guide tube. Certainly, inserting a tube enables retraction through the bending point. Thereby, retraction in a curved shape, as shown in Fig. 1, was also successful. Note that, these properties can also be applied to the conventional tip-extending robot which extends with increasing volume.

The phenomena explored in this study, such as buckling and bending, do not necessarily mean retraction failure but show that one degree of freedom can allow a variety of actions depending on the conditions. Namely, it can also be used as a function that can generate a large force to the bending point. If this function is applied, not only a search robot but also applications such as grippers and deployment mechanisms can be considered. In future work, we intend to establish the design policy of the guide tube and develop a branch structure.

Acknowledgment

We acknowledge financial support from JSPS KAKENHI under grants 18H05471.

Advice and comments given by Prof. Kajihara (Hokkaido University), Prof. Yamasaki (Yamashina Institute for Ornithology), and Ms. Hookabe (Hokkaido University) has been a great help in observation and taking picture of Nemertea.

References

[1] M. Mahvash and M. Zenati, “Toward a hybrid snake robot for single-port surgery,” in 2011 Annual International Conference of the IEEE Engineering in Medicine and Biology Society, Boston, MA, 2011, pp. 5372–5375,

[2] S. Hirose and H. Yamada, “Snake-like robots [Tutorial],” IEEE Robot. Automat. Mag., vol. 16, no. 1, pp. 88–98, Mar. 2009,

[3] J. C. McKenna et al., “Toroidal skin drive for snake robot locomotion,” in 2008 IEEE International Conference on Robotics and Automation, Pasadena, CA, USA, 2008, pp. 1150–1155,

[4] A. Horigome, H. Yamada, G. Endo, S. Sen, S. Hirose, and E. F. Fukushima, “Development of a coupled tendon-driven 3D multi-joint manipulator,” in 2014 IEEE International Conference on Robotics and Automation (ICRA), Hong Kong, China, 2014, pp. 5915–5920,

[5] M. Takeichi, K. Suzumori, G. Endo, and H. Nabae, “Development of Giacometti Arm With Balloon Body,” IEEE Robot. Autom. Lett., vol. 2, no. 2, pp. 951–957, Apr. 2017,

[6] S. Tadokoro et al., “Application of Active Scope Camera to forensic investigation of construction accident,” in 2009 IEEE Workshop on Advanced Robotics and its Social Impacts, Tokyo, Japan, 2009, pp. 47–50,

[7] K. Hatazaki, M. Konyo, K. Isaki, S. Tadokoro, F. Takemura, "Active scope camera for urban search and rescue", 2007 IEEE/RSJ International Conference on Intelligent Robots and Systems, San Diego, CA, USA, 2007, pp. 2596–2602,

[8] K. Hosaka, H. Tsukagoshi, and A. Kitagawa, “MOBILE ROBOT BY A DRAWING-OUT TYPE ACTUATOR FOR SMOOTH LOCOMOTION INSHIDE NARROW AND CURVING PIPES,” Proceedings of the 8th JFPS International Symposium on Fluid Power, OKINAWA 2011Oct. 25-28, 2011 p. 6, 2011.

[9] H. Tsukagoshi, A. Kitagawa, and M. Segawa, “Active Hose: an artificial elephant’s nose with maneuverability for rescue operation,” in Proceedings 2001 ICRA, Seoul, South Korea, 2001, vol. 3, pp. 2454–2459,

[10] E. W. Hawkes, L. H. Blumenschein, J. D. Greer, and A. M. Okamura, “A soft robot that navigates its environment through growth,” Sci. Robot., vol. 2, no. 8, p. eaan3028, Jul. 2017,

[11] J. D. Greer, T. K. Morimoto, A. M. Okamura, and E. W. Hawkes, “A Soft, Steerable Continuum Robot That Grows via Tip Extension,” Soft Robotics, vol. 6, no. 1, pp. 95–108, Feb. 2019,

[12] K. Tadakuma et al., “Nemertea Proboscis Inspired Extendable Mechanism,” 30th 2019 International Symposium on Micro-Nano Mechatronics and Human Science , Dec.1-4, 2019.

[13] L. H. Blumenschein, L. T. Gan, J. A. Fan, A. M. Okamura, and E. W. Hawkes, “A Tip-Extending Soft Robot Enables Reconfigurable and Deployable Antennas,” IEEE Robot. Autom. Lett., vol. 3, no. 2, pp. 949–956, Apr. 2018

[14] C. Lucarotti, M. Totaro, A. Sadeghi, B. Mazzolai, and L. Beccai, “Revealing bending and force in a soft body through a plant root inspired approach,” Sci Rep, vol. 5, no. 1, p. 8788, Aug. 2015

[15] R. Gibson, “A NEW GENUS AND SPECIES OF LINEID HETERONEMERTEAN FROM SOUTH AFRICA, POLYBRACHIORHYNCHUS DAYI (NEMERTEA: ANOPLA), POSSESSING A MULTI- BRANCHED PROBOSCIS,” BULLETIN OF MARINE SCIENCE, vol. 27, p. 20, 1977.

[16] H. Kajihara, “A histology-free description of the branched-proboscis ribbonworm Gorgonorhynchus albocinctus sp. nov. (Nemertea: Heteronemertea),” Publ. Seto Mar. Biol. Lab., 43: 92–102, 2015

[17] Animal Wire/”ALIEN WORM SHOOTS GOOEY WEB”: In Initial Caps. (May, 15, 2015). Accessed:Feb. 22, 2020. [Online Video]. Available:https://www.youtube.com/watch?v=MmGz8gotCPs

[18] "AVID TV. Nemertea marine ribbon worm / น่าคลัง หนอนทะเล เป็นแบบนี้ In Initial Caps. (June. 3. 2015). Accessed : November. 8. 2019 [Online Video]. Available: https://www.youtube.com/watch?v=ez4l514lBb8"

[19] M. M. Coad, R. P. Thomasson, L. H. Blumenschein, N. S. Usevitch, E. W. Hawkes, and A. M. Okamura, “Retraction of Soft Growing Robots without Buckling,” IEEE Robot. Autom. Lett., pp. 1–1, 2020,

[20] S.-G. Jeong et al., “A Tip Mount for Carrying Payloads using Soft Growing Robots,” arXiv:1912.08297 [cs], Dec. 2019.

[21] J. Luong et al., “Eversion and Retraction of a Soft Robot Towards the Exploration of Coral Reefs,” in 2019 2nd IEEE International Conference on Soft Robotics (RoboSoft), Seoul, Korea (South), 2019, pp. 801–807,

[22] Li, H., Yao, J., Liu, C., Zhou, P., Xu, Y., and Zhao, Y. (2020). A bioinspired soft swallowing robot based on compliant guiding structure. Soft Robotics

[23] R. Comer and S. Levy, “Deflections of an inflated circular-cylindrical cantilever beam,” Amer. Inst. Aeronaut. Astronaut. J., vol. 1, no. 7, pp. 1652–1655, 1963.

[24] R.W. Leonard, G.W. Brooks, and H.G. McComb Jr, “Structural considerations of inflatable reentry vehicles,” Nat. Air Space Admin.Tech. Note, vol. 457, pp. 1–23, 1960.

[25] -W. Fichter, “A theory for inflated thin-wall cylindrical beams,” Nat. Air Space Admin. Tech. Note, vol. 3466, pp. 1–19, 1966.

[26] D. A. Haggerty, N. D. Naclerio, and E. W. Hawkes, “Characterizing environmental interactions for soft growing robots,” 2019 And an additional reference that demonstrate branched structures

[27] A. Le-van and C. Wielgosz, “Bending and buckling of inflatable beams:Some new theoretical results,” Thin-Walled Struct., vol. 43, no. 8, pp.1166–1187, 2005.

[28] M. Watanabe, K. Tadakuma, M. Konyo, and S. Tadokoro, “Bundled Rotary Helix Drive Mechanism Capable of Smooth Peristaltic Movement,” IEEE Robot. Autom. Lett., pp. 1–1, 2020,